Metrol. Meas. Syst., Vol. 29 (2022), No. 2
DOI: 10.24425/mms.2022.140029

METROLOGY AND MEASUREMENT SYSTEMS
Index 330930, ISSN 0860-8229
www.metrology.wat.edu.pl

MEASUREMENT AND THREE-DIMENSIONAL CALCULATION OF INDUCED ELECTROMOTIVE FORCE IN PERMANENT MAGNETS HEATER CYLINDERS

Riad Bouakacha[1)], Mehdi Ouili[2)], Hicham Allag[1)], Rabia Mehasni[2)], Mohammed Chebout[3)], Houssem Rafik Al-hana Bouchekara[4)]

1) *L2EI laboratory, University of Jijel,18000, Algeria* (*r.bouakacha@yahoo.fr*, *allag.hicham@univ-jijel.dz*)
2) *LEC laboratory, University of Constantine1, Algeria* (*ouili.mehdi@yahoo.fr*, *mehasni@yahoo.fr*)
3) *L2ADI Applied Automation and Industrial Diagnostics Laboratory, University of Djelfa, Algeria* (✉ *m.chebout@univ-djelfa.dz*, +213 791 737 258)
4) *Electrical Engineering, University of Hafr Al Batin, Saudi Arabia* (*bouchekara.houssem@gmail.com*)

Abstract

In this work, the electromotive force (EMF) near a permanent magnet heating cylinder was determined using a practical test bench. The aim is to elaborate three-dimensional analytical calculation capable of predicting accurately the same electromagnetic quantities by calculating the induced EMF in the presence of an inductive sensor. The analytical approach is obtained from developing mathematical integrals using the Coulombian approach to permanent magnets. In this approach, rotations are considered by Euler's transformations matrices permitting the calculation of all permanent magnets flux densities contributions at the same points in the surrounding free space. These points, part of a uniform rectangular grid of the active EMF sensor surface, are used to compute the EMF by Faraday's law. The validation results between experimental and simulated ones confirm the robustness and the efficiency of the proposed analytical approach.

Keywords: electromotive force (EMF), induction heating, permanent magnet, EMF sensor.

1. Introduction

The magnitude of the *electromotive force* (EMF) presents an essential research subject in the field of electrical engineering, mostly in the development of high throughput techniques, solar energy, photo-catalysis, high temperature systems and solid-state electrolytes [1]. There are several works which are based on EMF calculation, in particular in the field of electrical machines for diagnosis [2], optimization [3], control [4] and measurements (speed torque) [5]. Furthermore, EMF plays a very important role in the field of electrical engineering and it is one of the electromagnetic quantities for which various special sensors have been manufactured. Existing EMF sensors are safe, reliable, robust and can be used in extreme conditions. In the majority of cases, they are used to retrieve information and test the performances of systems before final manufacture. Concerning classical induction heating devices which are generally composed of hollow copper inductors allowing the flow of cooling fluid and metal armature parts to be heated located inside these inductors or close to them. The essential parameters in induction heating are the strong supply currents and the high applied frequencies. These heaters are known by their low efficiencies, about 45 % of the power is transmitted and the rest is lost as the Joule heating effect. The researchers tried to increase the efficiency by optimizing the shape of the inductors but they managed to earn only 10% [6]. Other researchers have thought about the use of rare earth permanent magnets, which occur significant magnetic field intensities. In this manner, to induce eddy currents, the users are forced to permanently move

Article history: received October 15, 2021; revised December 20, 2021; accepted December 29, 2021; available online April 6, 2022.

the magnets or the pieces to be heated. The experimental results permit to confirm that permanent magnet heater prototypes give excellent process quality with minimal energy consumption when compared to conventional AC heaters. Moreover, permanent magnet devices contribute to increase in efficiency (from 50% to more than 70%) allowing not only to reduce the cost of energy used but also leading to positive on environment, as demonstrated in [6]. The real problem are always the magnets demagnetization risks at high temperatures [6-9], in this case, contrary to magnetic refrigeration systems, permanent magnets must be thermally insulated. Refrigeration with the use of permanents magnets of materials has been largely used for the last ten years [10], but the competitiveness seems in favor of superconductor materials because of their strong magnetic fields, permitting large cooling power applications [11-12].

Recent developments in permanent magnets induction heating systems are very promising for relatively mean power ranges. Special attention is given to heating of nonmagnetic cylindrical billets in an alternating magnetic field created with permanent magnets rotating systems [13-14]. Unusual disposition of permanent magnets is important to amplify the magnetic effect. In this way, an alternative arrangement of permanent magnets with a constant rotation speed is needed for sinusoidal waveform heating. These arrangements were generally inspired by linear Halbach configurations [13-19]. Cylindrical Halbach arrays are emerging as competitive magnet structures for permanent magnet type eddy current heating. Other works investigate the use of the permanent magnet type eddy current heating method based on cylindrical Halbach arrays to reduce the viscosity of crude oil in oil wells [19]. Several modelling and simulation works have been realized to observe the performances of these kinds of devices and the *finite elements method* (FEM) is the most applicable numerical approach [19-21]. Used for bi-dimensional or three-dimensional configurations, FEM needs meshes for all significant electromagnetic regions and the surrounding air space. Moreover, in the presence of any movements, meshes must be partially or globally renewed at every displacement step, causing large time costs and possible CPU memory saturation. To avoid these situations, we have developed in this work a three-dimensional analytical model for permanent magnets from quasi-static Green's functions executed in the Coulombian approach [22-27]. The most important assumption of the Coulombian approach is taking into consideration constant magnetizations developed by permanent magnets. This is possible for all modern manufactured permanents magnet and especially the rare-earth element ones. Analytical developments are possible for parallelepipedic permanent magnets shapes [22-27]. Furthermore, we do not need any meshes in the surrounding spaces and the total implementation is suitable for any programming codes. After developing magnetic flux density expressions for any space points surrounding cuboidal permanent magnets, the electromotive force can be expressed and calculated for the active EMF sensor surface under consideration. The calculations will be performed for respectively four and eight permanent magnet arrangements and validated by practical results.

2. Problem description

The test bench has been made in the Laboratory of Electrical Engineering of Constantine 1 University. The bench consists of two electrical motors working in fixed or variable speeds modes, controlled, and powered by power inverters. We use an EMF inductive sensor of 1600 turns to measure the EMF with one signal analyser apparatus. The permanent magnets are mounted on the external surface of the cylinder drum (heater cylinder) as shown in Fig. 1.

Metrol. Meas. Syst., Vol. 29 (2022), No. 2
DOI: 10.24425/mms.2022.140029

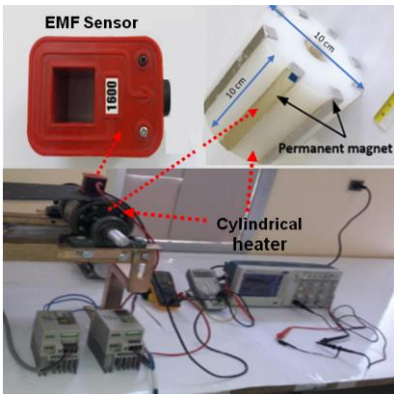

Fig. 1. Practical test bench.

The cylinder heater is rotated with constant speed and the generated voltage in nearby EMF sensor is then observed. The sensor is placed at the top of the heater cylinder as shown in Fig. 2. A maximum of eight permanent magnets can be placed on the cylinder. These magnets are mounted to create alternatively radial magnetizations. The number of permanent magnets can be easily reduced to four, but the magnetization of the magnets must be alternated to amplify the frequency of the induced flux densities. The electromagnetic system dimensions, distances and physical parameters are shown in Table 1.

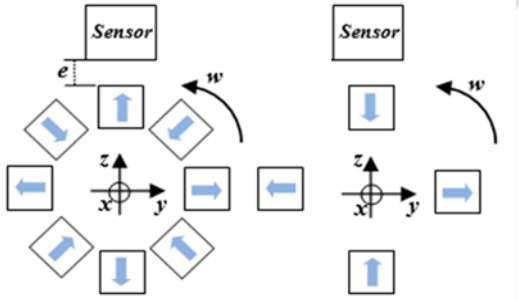

Fig. 2. Proposed configurations.

Table 1. Dimensions and parameters Data.

Magnet	Half length of PM a	Half width of PM b	Half height of PM c	Polarization of PM J
	50 mm	6 mm	5 mm	1.2 T
Heater	Radius R	Rotation speed w	Air gap length e	
	45 mm	20×2π rad/s	2 mm	

3. Analytical Developments

3.1. Magnetic flux density calculation

The Coulombian approach to parallelepipedal permanent magnets is used here [18, 22-27]. Each cuboidal magnet is replaced by two equivalent opposite charged surfaces as shown in Fig. 3. The concerned surfaces considered have always their normal vectors parallel to the magnetization one. In our case, the magnetization is along the *Z* axis, leading us to consider the two surfaces in the *XY*- plane. This charge density, indicated by σ, is equivalent to magnetic polarization J and proportional to magnetization M_p:

$$\sigma = J = \mu_0 M_p. \tag{1}$$

The origin of the (*x*, *y*, *z*) axes is assumed at the center of the permanent magnet with the following dimensions: 2a=10 cm, 2b=1.2 cm and 2c=1 cm. The calculation point is localized by the distances (α, β and γ) according respectively to (*x*, *y*, and *z*) axes.

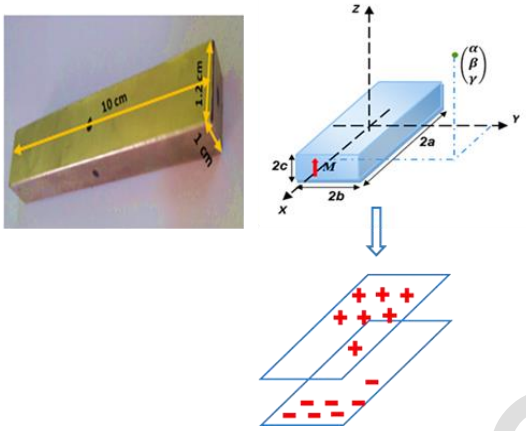

Fig. 3. Charged-surfaces model of permanent magnet.

To configure the permanent magnets heater cylinder, we first assume that the rotation along *X*-axis and all the permanent magnets magnetizations that are oriented in the inclined Z_n axes respecting ($n = 1 \ldots N$), where N is the total number of permanent magnets, θ is the rotation angle and $\Delta\theta$ is the fixed angular distance between adjacent permanent magnets as given in the following expression:

$$\Delta\theta = \frac{2\pi}{N} . \tag{2}$$

The real position of any permanent magnet (n) is given in:

$$\theta_n = \theta + (n-1)\cdot\Delta\theta . \tag{3}$$

To consider all permanent magnets in the same calculation, we should start from a fixed global coordinate system (*X*, *Y*, *Z*) located in the center of the cylinder. The local axes are those located in the centers of cuboid permanent magnets. Each local coordinate system is inclined by its θ_n angle according to the *x*-direction as shown in Fig. 4.

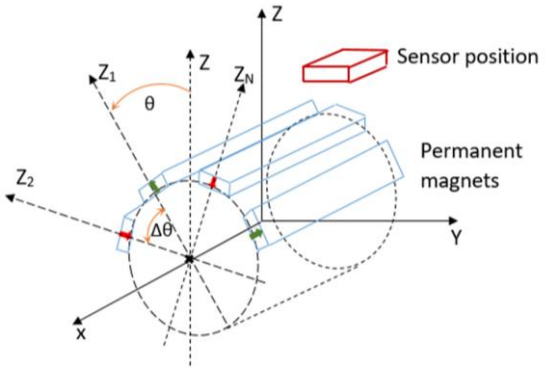

Fig. 4. Three-dimensional system configuration.

The relationship between local rotary axes and global axes is defined by Euler's transformation matrices. The transformation matrix (with Euler's transformation used for only *X*-axis) is as follows:

$$T_n = \begin{bmatrix} 1 & 0 & 0 \\ 0 & cos\,\theta_n & -sin\,\theta_n \\ 0 & sin\,\theta_n & cos\,\theta_n \end{bmatrix}. \tag{4}$$

The calculating point (α, β, γ), defined in the global coordinate system must be separately expressed in all the local coordinates as follows:

$$\begin{bmatrix} \alpha_n \\ \beta_n \\ \gamma_n \end{bmatrix} = \begin{bmatrix} 1 & 0 & 0 \\ 0 & cos\,\theta_n & -sin\,\theta_n \\ 0 & sin\,\theta_n & cos\,\theta_n \end{bmatrix} \cdot \begin{bmatrix} \alpha \\ \beta \\ \gamma \end{bmatrix} - \begin{bmatrix} 0 \\ 0 \\ R \end{bmatrix}, \tag{5}$$

where: R is the radius of the cylinder, identical to the distance separating the center of the global coordinate system and the local ones located at the center of each permanent magnet. The expressions of magnetic flux density components at the calculating points are given as in [18, 21-22]. With respect to (α_n, β_n and γ_n), the equations of flux densities are as follows:

$$Bn_x = \frac{\sigma}{4\pi}\sum_{k=0}^{1}\sum_{i=0}^{1}\sum_{j=0}^{1}(-1)^{i+j+k}\,ln(r-V), \tag{6}$$

$$Bn_y = \frac{\sigma}{4\pi}\sum_{k=0}^{1}\sum_{i=0}^{1}\sum_{j=0}^{1}(-1)^{i+j+k}\,ln(r-U), \tag{7}$$

$$Bn_z = \frac{\sigma}{4\pi}\sum_{k=0}^{1}\sum_{i=0}^{1}\sum_{j=0}^{1}(-1)^{i+j+k}\,tg^{-1}\left(\frac{UV}{Wr}\right). \tag{8}$$

The variables *U*,*V* and *W* are as follows:

$$\begin{cases} U = \alpha_n - (-1)^i a \\ V = \beta_n - (-1)^j b \\ W = \gamma_n - (-1)^k c \\ r = \sqrt{U^2 + V^2 + W^2} \end{cases}. \tag{9}$$

After defining all magnetic induction components in their specific axes for all the magnets, starting from the first ($n = 1$) to the last ($n = N$), components in the global axes (X, Y, Z) must be expressed to superpose them.

$$\begin{bmatrix} B_x \\ B_y \\ B_z \end{bmatrix} = \sum_{n=1}^{N}(-1)^n \begin{bmatrix} 1 & 0 & 0 \\ 0 & cos\,\theta_n & sin\,\theta_n \\ 0 & -sin\,\theta_n & cos\,\theta_n \end{bmatrix} \cdot \begin{bmatrix} Bn_x \\ Bn_y \\ Bn_z \end{bmatrix} = \sum_{n=1}^{N}(-1)^n T_n^{-1} \cdot \begin{bmatrix} Bn_x \\ Bn_y \\ Bn_z \end{bmatrix}. \tag{10}$$

The $(-1)^n$ term represents the alternative effect of magnetization.

3.2. EMF calculation

To calculate the induced EMF from the magnetic flux density over the EMF sensor surface, Faraday's law is applied as follows:

$$E = -N_t\frac{d\varphi}{dt} = -N_t\frac{d}{dt}\iint_S B\cdot dS = -N_t\frac{d\theta}{dt}\frac{d}{d\theta}\iint_S B\cdot dS, \tag{11}$$

where N_t is the number of turns, and the variable speed is presented by $d\theta/dt$.

To avoid direct integral calculations, which are very hard and may prove analytically impossible, the entire surface is decomposed to several small ones, in which the magnetic flux density variations can be neglected. According to the shape of the EMF sensor active surface, a rectangular grid can be used as shown in Fig. 5.

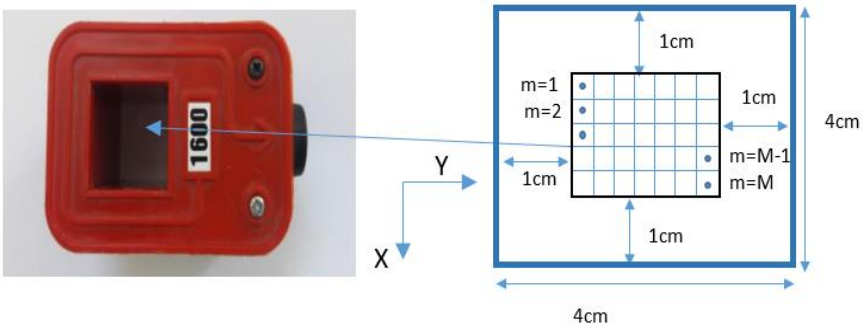

Fig. 5. Decomposed rectangular active surface for the EMF sensor.

Let us consider *M*, the total number of all small rectangular surfaces. In this case, (11) can be written as:

$$E = -N_t \frac{d\theta}{dt} \sum_{m=1}^{M} B_m . dS_m . \tag{12}$$

In the case of constant speed, the following expression can be given:

$$\Omega = \frac{d\theta}{dt} = cst \tag{13}$$

Below, the normal vector of the active surface for the sensor is oriented in the *Z* direction. We can simply write:

$$E = -N_t \Omega \cdot \sum_{m=1}^{M} Bm_z dS_m . \tag{14}$$

From equation (10), each flux density component can be expressed as:

$$B_{mz} = \sum_{n=1}^{N} \left(-sin\,\theta_n \cdot Bn_y + cos\,\theta_n \cdot Bn_z \right), \tag{15}$$

where Bn_y and Bn_z are same as the components developed in (7-8). The only changes are in the expressions of variables *U*, *V*, and *W*:

$$\begin{aligned} U &= \alpha_n - \alpha_m - (-1)^i a \\ V &= \beta_n - \beta_m - (-1)^j b \\ W &= \gamma_n - \gamma_m - (-1)^k c \end{aligned} , \tag{16}$$

where (α_m, β_m, and γ_m) are the space coordinates of the centers of all elements of the rectangular grid of active surface considered for the EMF sensor, Fig. 5.

4. Calculations and experimental validation

The developed approach has been applied to two cases studies. In the first case there are 8 alternating magnets (maximum possible number of magnets), whilst in the second one study, there are 4 alternating magnets.

Analytical calculations are implemented in the commercial MATLAB programming software. The tridimensional configuration is shown by respective dimensions and the geometry of the studied system using the patch objects proposed by the same software. Consequently, we demonstrate the two investigated configurations in Fig. 6 and Fig. 7.

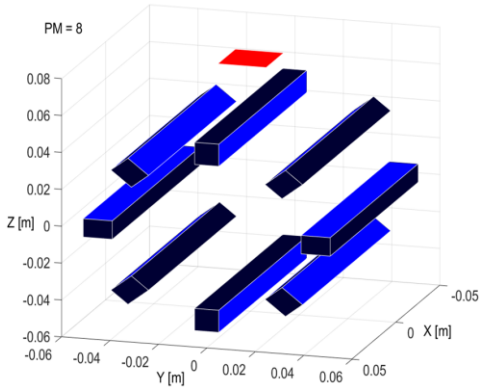

Fig. 6. Eight-PM arrangement.

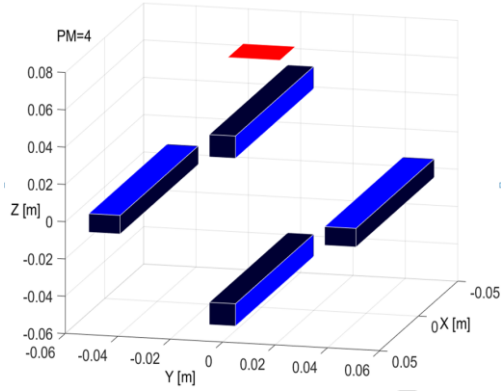

Fig. 7. Four-PM arrangement.

The rotation speed is chosen as 20 round/s thus, in this case, we observe the *magnetic flux densities* (MFD) on the active surface of the EMF sensor. This sensor is square-shaped (2cm×2cm) and can be composed of several small surfaces following an imposed linear grid pattern. Next, results are obtained for respectively (*M=60*) total surface elements Fig. 5. In Fig. 8, at $\theta = 0°$, the sensor is situated above the first permanent magnet. This position presents a perfect symmetric configuration. Contrarily, at $\theta = 30°$, which is an arbitrary position Fig. 9.

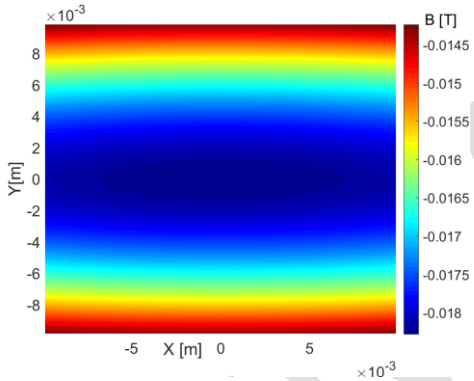

Fig. 8. MFD on the active surface of EMF sensor for the eight-PM configuration at $\theta = 0°$.

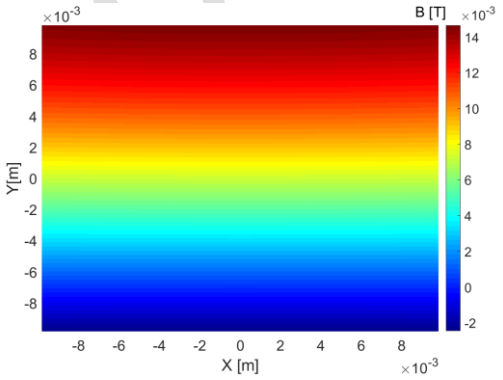

Fig. 9. MFD on the active surface of EMF sensor for the eight-PM configuration at $\theta = 30°$.

In the MATLAB programming code, the manipulation of matrices, element-by-element multiplications or divisions are very fast and suitable techniques. In other words, with a good using and for skillful programmers, the number of surface elements affect hardly the time cost and considerably increase the precision and the quality. These advantages are in favor of numerical integration calculations of EMF. For a complete rotation of the cylinder at 20 round/s, the total time is 0.05 s. In this case, we present the results of calculating the magnetic flux (in *Weber*) and the electromotive force (in *Volt*) for the four- and eight-permanent magnet configurations, Fig. 10 and Fig. 11.

From these results, we can perfectly see that the EMF form is similar to the negative derivative of the magnetic flux. The measured EMF signals, given by the analyzer for the same considerations, are compared to those calculated analytically in Fig. 12 and Fig. 13. The resulting curves look excellent with only a few accepted differences.

For these and other applications, such as Inductrack levitation [28], magnetic couplings [29], passive magnetic bearings [30], and permanent magnet undulators [31], the magnetic delivered by permanent magnet arrangements should be as close to the sinusoidal harmonic shapes as possible to avoid noise or vibration. EMF detection allows the effects of a magnetic field or flux density to be observed at close range.

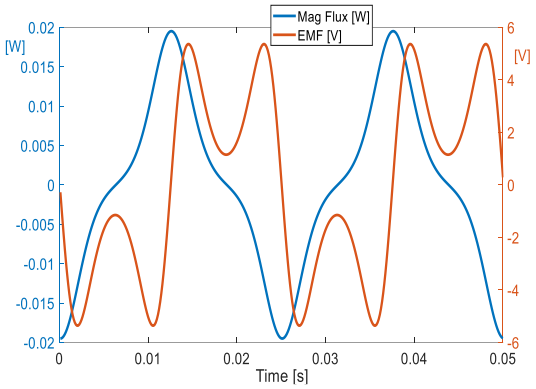

Fig. 10. Magnetic flux and EMF as a function of time for the four-PM arrangement.

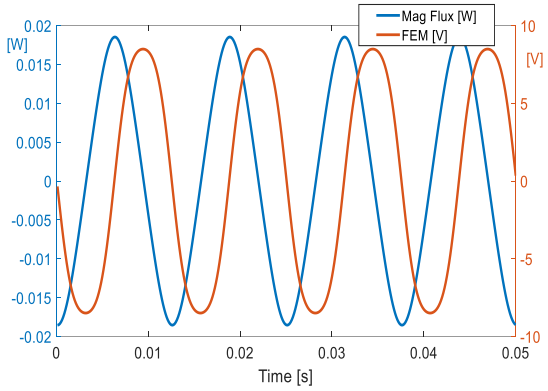

Fig. 11. Magnetic flux and EMF as a function of time for the eight-PM arrangement.

For the applied airgap (e=2mm), the best arrangement is that of eight permanent magnets, in which the FEM is purely sinusoidal. The use of the four-magnet configuration as a sinusoidal magnetic field source is possible, but for a much larger air gap leading to reduction of the intensity of magnetic fields.

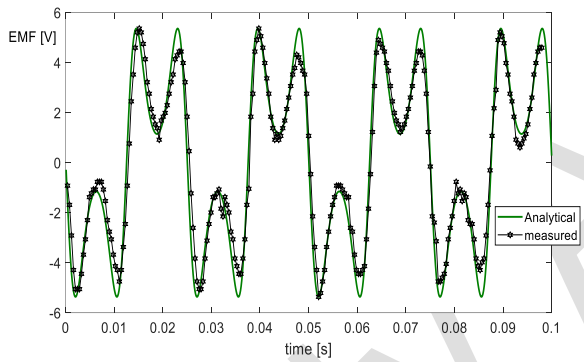

Fig. 12. Measured and calculated EMF for the four-PM configuration.

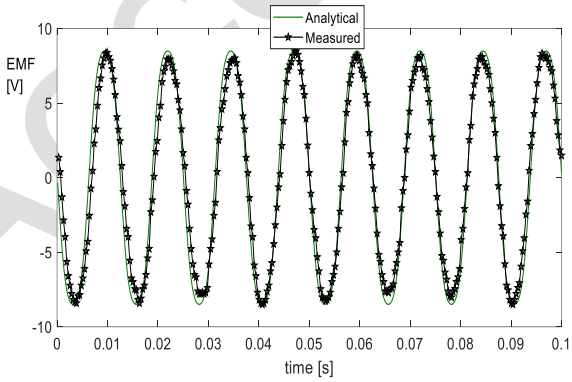

Fig. 13. Measured and calculated EMF for the eight PM configuration.

As can be seen in Fig. 12 and Fig. 13, the frequency of the EMF signals is always constant following the invariant rotation velocity of the cylinder. This kind of control is largely used in permanent magnet motors through observing the magnet's flux or the electromotive force (EMF) to detect the rotor's position information contained in these physical variables [32]. Still, in the same kind of applications, the average temperature of permanent magnets can also be estimated using *Back Electromotive Force* (BEMF) by analyzing the fundamental or higher-order harmonics [33]. The EMF measurements can be used to detect asymmetrical demagnetization defects by observing some irregularities in periodical signals which can easily be applied in our analytical approach by reducing the values of magnetization for some magnets. In [34], the results show the effectiveness of the EMF sensing technique. In real drive systems, this condition monitoring methodology can be applied to detect demagnetization problems at an early stage before large damage occurs, or as a virtual sensor to monitor the magnet temperature.

Table A.1 and Table A.2 shows the numerical values of measured and analytical results according to Fig. 6 for configurations with eight permanent magnets and for four permanent magnets in Fig. 7. In the third and fourth columns of the same table, absolute and relative errors have been given.

The calculated mean values and standard deviation from relative errors vectors for the two studied configurations are shown in Table 2.

Table 2. Statistical presentation of relative errors.

	Mean value	Standard deviation value
PM=4	0.1780	0.1329
PM = 8	0.0995	0.0782

It is always difficult to talk about the origin of errors, especially those resulting from measurements. However, in this specific case, we believe that these errors are due to the practical implemented conditions. In this situation, the controlled rotation speed of the heater cylinder ensured by the driving motor whose speed can slightly or unexpectedly decrease or increase compared to the reference fixed speed influences directly the periodicity of the measured signal. This influence contributes to increasing errors compared to analytical results that do not have this kind of problem. The sampling offered by the digital analyzer has its own limits notably in terms of precision. In other words, the number of measured values is limited and depends on the device used. We also notice that the mean of relative errors and the standard deviation values for the eight-PM system is lower than that for the four-PM one; we think that this is due to the inductive nature of this kind of sensor where the sensitivity increases with the variation of the magnetic field. In this case, the eight PM variant doubles the period of the magnetic field quantity and, consequently, the EMF-sensed signal compared to four-PM configurations. In addition, in this application some fluctuations at the peak values of t curves, in particular, for the four-PM arrangement, show that the magnets do not have precisely the same remnant magnetizations despite their being intended to have.

5. Conclusions

In this work, the EMF is measured and calculated, in order to test the performances of a designed permanent magnets heater cylinder and prove the efficiency of the three-dimensional Coulombian approach. The use of this analytical computing procedure is justified by its robustness, simplicity in programming, and its adaptability to modern industrial parallelepipedal permanent magnets of rigid magnetizations. There are significant technical novelties in this paper and the principal one is the use of Euler's transformations to superpose all the permanent magnets effects in only one point of calculation. Using the matrix manipulation techniques, the computation at several observation points is simultaneously realized, permitting very fast executions. Realizing and exploiting the experimental bench, we have succeeded to measure the EMF and demonstrated the strength of our approach by comparing the results for arrangements of four and the eight permanent magnets. From measured and analytical results, we can observe the periodicity of magnetic quantities developed by such applications. With these results, we can decide on the placement of the metal pieces to be heated and predict the shapes and the values of induced eddy currents (some results were published by our team on this subject [35]). On other hand, the analytical approach developed by us represents a good way for the optimization process and inverse problem analysis because all the expressions obtained are in direct relation with dimensions and physical parameters.

Acknowledgements

Funding was provided by the General Directorate of Research and Development Technologies/Ministry of Higher Education and Research Sciences DGRSDT/MERS, Algeria. Experimental equipment was provided by the LEC laboratory, University of Constantine 1, Algeria.

Appendices

Table A.1. Relative error calculation for four permanent magnets (PM=4).

Time [s]	Measured [V]	Calculated [V]	Absolute Error [V]	Relative Error	Time [s]	Measured [V]	Calculated [V]	Absolute Error [V]	Relative Error	Time [s]	Measured [V]	Calculated [V]	Absolute Error [V]	Relative Error
0.0004	-0.9169	-0.9368	0.0198	0.0037	0.0332	-1.6810	-3.1101	1.4291	0.2672	0.0660	3.9734	5.3229	1.9762	0.3695
0.0008	-1.6810	-2.6808	0.9998	0.1869	0.0336	-1.9867	-3.7821	1.7954	0.3357	0.0664	3.6677	5.0082	2.0589	0.3849
0.0012	-2.9036	-4.0694	1.1658	0.2180	0.0340	-2.7508	-4.4497	1.6990	0.3176	0.0668	3.0564	4.4497	1.7158	0.3208
0.0016	-4.2790	-4.9634	0.6844	0.1279	0.0344	-3.0564	-5.0082	1.9518	0.3649	0.0672	2.4451	3.7821	1.2551	0.2346
0.0021	-5.0431	-5.3324	0.2893	0.0541	0.0349	-3.8205	-5.3229	1.5023	0.2809	0.0677	1.9867	3.1101	0.8322	0.1556
0.0025	-5.0431	-5.2426	0.1995	0.0373	0.0353	-4.1262	-5.2531	1.1269	0.2107	0.0681	1.6810	2.5027	0.4481	0.0838
0.0029	-5.0431	-4.8197	0.2235	0.0418	0.0357	-4.4318	-4.6904	0.2586	0.0483	0.0685	1.5282	1.9971	0.1010	0.0189
0.0033	-4.4318	-4.2057	0.2261	0.0423	0.0361	-4.4318	-3.6015	0.8303	0.1552	0.0689	1.2226	1.6088	0.5178	0.0968
0.0037	-3.6677	-3.5261	0.1416	0.0265	0.0365	-3.8205	-2.0578	1.7628	0.3296	0.0693	1.3754	1.3406	0.7980	0.1492
0.0041	-3.0564	-2.8721	0.1843	0.0345	0.0369	-3.0564	-0.2355	2.8209	0.5274	0.0697	1.5282	1.1901	1.1917	0.2228
0.0045	-2.2923	-2.2999	0.0076	0.0014	0.0373	-1.6810	1.6195	3.3005	0.6171	0.0701	1.8339	1.1545	1.5236	0.2848
0.0049	-1.3754	-1.8374	0.4620	0.0864	0.0377	-1.0392	3.2530	4.2921	0.8025	0.0705	2.1395	1.2329	1.8983	0.3549
0.0053	-1.2226	-1.4942	0.2717	0.0508	0.0381	1.8339	4.4666	2.6328	0.4922	0.0709	2.5980	1.4272	2.0807	0.3890
0.0057	-1.0697	-1.2705	0.2008	0.0375	0.0385	2.7508	5.1615	2.4107	0.4507	0.0713	3.0564	1.7403	2.1061	0.3938
0.0062	-1.0697	-1.1634	0.0936	0.0175	0.0390	4.4318	5.3466	0.9148	0.1710	0.0718	3.6677	2.1734	1.6810	0.3143
0.0066	-0.7641	-1.1705	0.4064	0.0760	0.0394	4.8903	5.1154	0.2251	0.0421	0.0722	3.9734	2.7199	1.1303	0.2113
0.0070	-0.7641	-1.2921	0.5279	0.0987	0.0398	5.3487	4.6045	0.7443	0.1392	0.0726	4.4318	3.3574	0.0895	0.0167
0.0074	-0.7641	-1.5305	0.7664	0.1433	0.0402	5.0431	3.9529	1.0902	0.2038	0.0730	4.4318	4.0378	1.3633	0.2549
0.0078	-1.0697	-1.8888	0.8190	0.1531	0.0406	4.5846	3.2741	1.3105	0.2450	0.0734	4.2790	4.6787	2.8842	0.5392
0.0082	-1.5282	-2.3658	0.8376	0.1566	0.0410	3.9734	2.6460	1.3274	0.2482	0.0738	3.6677	5.1625	4.1382	0.7737
0.0086	-2.2923	-2.9503	0.6579	0.1230	0.0414	3.3621	2.1128	1.2492	0.2336	0.0742	2.7508	5.3487	5.0212	0.9388
0.0090	-2.7508	-3.6112	0.8604	0.1609	0.0418	2.7508	1.6946	1.0562	0.1975	0.0746	1.2226	5.1037	4.9876	0.9325
0.0094	-3.0564	-4.2884	1.2319	0.2303	0.0422	1.8339	1.3965	0.4374	0.0818	0.0750	-0.1528	4.3423	4.6369	0.8669
0.0098	-3.6677	-4.8858	1.2181	0.2277	0.0426	1.3754	1.2168	0.1585	0.0296	0.0754	-2.1395	3.0685	3.1476	0.5885
0.0103	-4.1262	-5.2750	1.1488	0.2148	0.0431	0.9169	1.1527	0.2358	0.0441	0.0759	-2.3865	1.3948	2.9153	0.5451
0.0107	-4.2790	-5.3135	1.0345	0.1934	0.0435	1.1462	1.2026	0.0564	0.0105	0.0763	-3.1328	-0.4705	1.8159	0.3395
0.0111	-4.7375	-4.8807	0.1433	0.0268	0.0439	0.9169	1.3676	0.4507	0.0843	0.0767	-4.7375	-2.2705	0.3677	0.0687
0.0115	-4.2790	-3.9211	0.3579	0.0669	0.0443	1.0697	1.6508	0.5810	0.1086	0.0771	-4.7375	-3.7650	1.0409	0.1946
0.0119	-3.3621	-2.4783	0.8838	0.1652	0.0447	1.3754	2.0541	0.6787	0.1269	0.0775	-4.5846	-4.7898	1.5550	0.2907
0.0123	-2.4451	-0.7044	1.7407	0.3254	0.0451	1.6810	2.5735	0.8925	0.1669	0.0779	-4.4318	-5.2871	1.9984	0.3736
0.0127	-0.9169	1.1671	2.0840	0.3896	0.0455	2.1395	3.1916	1.0521	0.1967	0.0783	-4.0345	-5.3018	2.0925	0.3912
0.0131	0.7641	2.8777	2.1136	0.3952	0.0459	2.5980	3.8676	1.2696	0.2374	0.0787	-3.0564	-4.9488	1.4877	0.2781
0.0135	2.4451	4.2099	1.7647	0.3299	0.0463	3.0564	4.5281	1.4716	0.2751	0.0791	-2.5980	-4.3698	1.2826	0.2398
0.0139	3.5149	5.0377	1.5228	0.2847	0.0467	3.5149	5.0638	1.5489	0.2896	0.0795	-2.1395	-3.6965	0.9601	0.1795
0.0144	4.5846	5.3441	0.7595	0.1420	0.0472	3.7769	5.3379	1.5610	0.2919	0.0800	-1.5282	-3.0296	0.3702	0.0692
0.0148	5.1959	5.2050	0.0091	0.0017	0.0476	4.3008	5.2113	0.9105	0.1702	0.0804	-0.7641	-2.4334	0.4867	0.0910
0.0152	5.3487	4.7505	0.5982	0.1118	0.0480	4.2026	4.5827	0.3801	0.0711	0.0808	-1.2226	-1.9420	0.2372	0.0443
0.0156	5.1959	4.1222	1.0738	0.2008	0.0484	3.9734	3.4307	0.5426	0.1015	0.0812	-1.0697	-1.5687	0.7182	0.1343
0.0160	4.7375	3.4415	1.2960	0.2423	0.0488	3.6677	1.8406	1.8271	0.3416	0.0816	-1.5282	-1.3154	0.7076	0.1323
0.0164	4.1262	2.7953	1.3308	0.2488	0.0492	3.5149	0.0000	3.5149	0.6571	0.0820	-1.2226	-1.1794	1.5728	0.2940
0.0168	3.2092	2.2358	0.9735	0.1820	0.0496	2.7508	-1.8406	4.5914	0.8584	0.0824	-1.3754	-1.1580	2.0661	0.3863
0.0172	2.7508	1.7879	0.9629	0.1800	0.0500	1.0697	-3.4307	4.5005	0.8414	0.0828	-2.2923	-1.2508	1.8298	0.3421
0.0176	2.1395	1.4598	0.6797	0.1271	0.0504	-0.4585	-4.5827	4.1242	0.7711	0.0832	-2.4451	-1.4598	2.3054	0.4310
0.0180	1.8339	1.2508	0.5830	0.1090	0.0508	-2.1395	-5.2113	3.0718	0.5743	0.0836	-2.4451	-1.7879	2.7599	0.5160
0.0185	1.5282	1.1580	0.3702	0.0692	0.0513	-3.3621	-5.3379	1.9758	0.3694	0.0841	-3.0564	-2.2358	2.2877	0.4277
0.0189	1.3754	1.1794	0.1960	0.0366	0.0517	-4.2790	-5.0638	0.7848	0.1467	0.0845	-3.8205	-2.7953	1.2171	0.2276
0.0193	0.9169	1.3154	0.3985	0.0745	0.0521	-5.3487	-4.5281	0.8207	0.1534	0.0849	-4.1262	-3.4415	0.0837	0.0157
0.0197	1.6810	1.5687	0.1123	0.0210	0.0525	-5.1959	-3.8676	1.3284	0.2484	0.0853	-4.2790	-4.1222	1.4013	0.2620
0.0201	1.8339	1.9420	0.1082	0.0202	0.0529	-4.7375	-3.1916	1.5458	0.2890	0.0857	-3.9734	-4.7505	2.8063	0.5247
0.0205	1.9867	2.4334	0.4467	0.0835	0.0533	-4.2790	-2.5735	1.7055	0.3189	0.0861	-3.8205	-5.2050	4.5249	0.8460
0.0209	2.2923	3.0296	0.7373	0.1378	0.0537	-3.3621	-2.0541	1.3080	0.2445	0.0865	-2.9036	-5.3441	5.3819	1.0062
0.0213	2.7508	3.6965	0.9457	0.1768	0.0541	-2.7508	-1.6508	1.1000	0.2057	0.0869	-1.6810	-5.0377	5.6021	1.0474
0.0217	3.2092	4.3698	1.1605	0.2170	0.0545	-2.1395	-1.3676	0.7719	0.1443	0.0873	-0.3056	-4.2099	5.1864	0.9696
0.0221	3.5149	4.9488	1.4339	0.2681	0.0549	-1.6810	-1.2026	0.4785	0.0895	0.0877	1.0697	-2.8777	4.2437	0.7934
0.0226	4.1262	5.3018	1.1756	0.2198	0.0554	-1.3754	-1.1527	0.2227	0.0416	0.0882	2.1701	-1.1671	3.1049	0.5805
0.0230	4.2790	5.2871	1.0081	0.1885	0.0558	-0.9169	-1.2168	0.2999	0.0561	0.0886	2.9036	0.7044	1.9822	0.3706
0.0234	4.4318	4.7898	0.3579	0.0669	0.0562	-0.9169	-1.3965	0.4795	0.0897	0.0890	4.8903	2.4783	0.6019	0.1125
0.0238	4.4318	3.7650	0.6668	0.1247	0.0566	-0.9169	-1.6946	0.7777	0.1454	0.0894	5.1959	3.9211	1.5848	0.2963
0.0242	3.9734	2.2705	1.7029	0.3184	0.0570	-1.0697	-2.1128	1.0431	0.1950	0.0898	5.0431	4.8807	2.0929	0.3913
0.0246	3.2092	0.4705	2.7388	0.5120	0.0574	-1.2226	-2.6460	1.4234	0.2661	0.0902	4.7652	5.3135	2.3994	0.4486
0.0250	1.8339	-1.3948	3.2287	0.6036	0.0578	-1.3754	-3.2741	1.8987	0.3550	0.0906	3.9734	5.2750	2.0846	0.3897
0.0254	0.4585	-3.0685	3.5270	0.6594	0.0582	-1.3754	-3.9529	2.5775	0.4819	0.0910	3.5149	4.8858	1.9843	0.3710
0.0258	-1.2226	-4.3423	3.1198	0.5833	0.0586	-2.5980	-4.6045	2.0065	0.3751	0.0914	2.7508	4.2884	1.4587	0.2727
0.0262	-2.5980	-5.1037	2.5057	0.4685	0.0590	-2.7508	-5.1154	2.3646	0.4421	0.0918	2.4451	3.6112	1.2747	0.2383
0.0267	-3.8205	-5.3487	1.5282	0.2857	0.0595	-3.6677	-5.3466	1.6789	0.3139	0.0923	1.8339	2.9503	0.6705	0.1254
0.0271	-4.7375	-5.1625	0.4251	0.0795	0.0599	-4.2790	-5.1615	0.8825	0.1650	0.0927	0.9169	2.3658	0.3536	0.0661
0.0275	-5.0431	-4.6787	0.3644	0.0681	0.0603	-4.4318	-4.4666	0.0348	0.0065	0.0931	0.7641	1.8888	0.7301	0.1365
0.0279	-5.0431	-4.0378	1.0053	0.1880	0.0607	-4.4318	-3.2530	1.1789	0.2204	0.0935	0.6113	1.5305	1.2261	0.2292
0.0283	-4.7375	-3.3574	1.3800	0.2580	0.0611	-4.2790	-1.6195	2.6595	0.4972	0.0939	0.7641	1.2921	1.5358	0.2871
0.0287	-3.8205	-2.7199	1.1006	0.2058	0.0615	-4.1262	0.2355	4.3617	0.8155	0.0943	0.9679	1.1705	1.9043	0.3560
0.0291	-3.1075	-2.1734	0.9341	0.1746	0.0619	-3.0564	2.0578	5.1142	0.9561	0.0947	1.1462	1.1634	2.3799	0.4450
0.0295	-2.4451	-1.7403	0.7048	0.1318	0.0623	-1.8339	3.6015	5.4353	1.0162	0.0951	1.5282	1.2705	2.6775	0.5006
0.0299	-1.9867	-1.4272	0.5595	0.1046	0.0627	-0.4585	4.6904	5.1489	0.9626	0.0955	2.1395	1.4942	2.6802	0.5011
0.0303	-1.3754	-1.2329	0.1425	0.0266	0.0631	1.2226	2.8721	4.0305	0.7535	0.0959	2.5980	1.8374	2.6447	0.4944
0.0308	-1.3754	-1.1545	0.2209	0.0413	0.0636	3.0564	3.5261	2.2664	0.4237	0.0964	3.5149	2.2999	1.8175	0.3398
0.0312	-1.2226	-1.1901	0.0325	0.0061	0.0640	4.3881	4.2057	0.6200	0.1159	0.0968	3.9734	4.9634	0.9900	0.1851
0.0316	1.0697	-1.3406	0.2708	0.0506	0.0644	4.8903	4.8197	0.4405	0.0824	0.0972	4.4318	4.0694	0.3624	0.0678
0.0320	-1.8339	-1.6088	0.2250	0.0421	0.0648	4.7375	5.2426	0.9554	0.1786	0.0976	4.5846	2.6808	1.9038	0.3559
0.0324	-2.1395	-1.9971	0.1424	0.0266	0.0652	4.5846	5.3324	1.4746	0.2757	0.0980	4.5846	0.9368	3.6479	0.6820
0.0328	-1.3754	-2.5027	1.1273	0.2108	0.0656	4.4318	5.2531	1.9292	0.3607					

Metrol. Meas. Syst., Vol. 29 (2022), No. 2
DOI: 10.24425/mms.2022.140029

Table A.2. Relative error calculation for eight permanent magnets (PM=8).

Time [s]	Meas. [V]	Calc. [V]	Abs. Error [V]	Relative Error	Time [s]	Meas. [V]	Calc. [V]	Abs. Error [V]	Relative Error	Time [s]	Meas. [V]	Calc. [V]	Abs. Error [V]	Relative Error	Time [s]	Meas. [V]	Calc. [V]	Abs. Error [V]	Relative Error
0.0003	1.3483	-0.8819	2.2302	0.2628	0.0253	0.7931	-0.8819	1.6750	0.1974	0.0503	-1.0568	-0.8819	0.1749	0.0206	0.0753	-1.2690	-0.8819	0.3871	0.0456
0.0006	0.3863	-2.5919	2.9782	0.3509	0.0256	-0.8724	-2.5919	1.7195	0.2026	0.0506	-2.1668	-2.5919	0.4251	0.0501	0.0756	-2.3001	-2.5919	0.2919	0.0344
0.0010	-1.2974	-4.1494	2.8520	0.3361	0.0260	-1.7890	-4.1494	2.3604	0.2781	0.0510	-3.4898	-4.1494	0.6596	0.0777	0.0760	-3.7277	-4.1494	0.4217	0.0497
0.0013	-2.8553	-5.4799	2.6246	0.3093	0.0263	-3.4105	-5.4799	2.0694	0.2439	0.0513	-4.0450	-5.4799	1.4349	0.1691	0.0763	-5.2347	-5.4799	0.2452	0.0289
0.0016	-3.9656	-6.5432	2.5775	0.3037	0.0266	-4.7588	-6.5432	1.7844	0.2103	0.0516	-5.3140	-6.5432	1.2292	0.1448	0.0766	-5.5519	-6.5432	0.9913	0.1168
0.0019	-5.6312	-7.3348	1.7036	0.2007	0.0269	-5.7898	-7.3348	1.5450	0.1821	0.0519	-6.2657	-7.3348	1.0691	0.1260	0.0769	-6.3450	-7.3348	0.9898	0.1166
0.0022	-6.5830	-7.8804	1.2974	0.1529	0.0272	-6.5037	-7.8804	1.3767	0.1622	0.0522	-7.4554	-7.8804	0.4250	0.0501	0.0772	-6.8209	-7.8804	1.0595	0.1248
0.0026	-7.2175	-8.2238	1.0063	0.1186	0.0276	-6.6623	-8.2238	1.5615	0.1840	0.0526	-8.0106	-8.2238	0.2132	0.0251	0.0776	-7.6140	-8.2238	0.6097	0.0718
0.0029	-7.7727	-8.4130	0.6404	0.0755	0.0279	-7.6140	-8.4130	0.7990	0.0941	0.0529	-8.0899	-8.4130	0.3231	0.0381	0.0779	-7.9313	-8.4130	0.4817	0.0568
0.0032	-8.1692	-8.4865	0.3173	0.0374	0.0282	-7.7727	-8.4865	0.7138	0.0841	0.0532	-8.2485	-8.4865	0.2379	0.0280	0.0782	-8.0106	-8.4865	0.4759	0.0561
0.0035	-8.3279	-8.4625	0.1347	0.0159	0.0285	-7.7727	-8.4625	0.6899	0.0813	0.0535	-8.1692	-8.4625	0.2933	0.0346	0.0785	-7.6140	-8.4625	0.8485	0.1000
0.0038	-8.4072	-8.3349	0.0723	0.0085	0.0288	-7.6934	-8.3349	0.6415	0.0756	0.0538	-8.0106	-8.3349	0.3243	0.0382	0.0788	-7.4554	-8.3349	0.8795	0.1036
0.0042	-7.9313	-8.0743	0.1430	0.0168	0.0292	-7.7727	-8.0743	0.3016	0.0355	0.0542	-2.2620	-8.0743	0.3809	0.0449	0.0792	-6.9795	-8.0743	1.0947	0.1290
0.0045	-7.8520	-7.6359	0.2161	0.0255	0.0295	-7.6934	-7.6359	0.0575	0.0068	0.0545	-0.6345	-7.6359	0.6563	0.0773	0.0795	-6.6623	-7.6359	0.9736	0.1147
0.0048	-7.2175	-6.9720	0.2455	0.0289	0.0298	-7.3761	-6.9720	0.4041	0.0476	0.0548	0.3173	-6.9720	0.4683	0.0552	0.0798	-6.1071	-6.9720	0.8649	0.1019
0.0051	-6.7416	-6.0460	0.6956	0.0820	0.0301	-5.8021	-6.0460	0.2440	0.0287	0.0551	2.3794	-6.0460	0.0976	0.0115	0.0801	-4.1692	-6.0460	1.8769	0.2212
0.0054	-6.1071	-4.8464	1.2607	0.1486	0.0304	-4.7588	-4.8464	0.0876	0.0103	0.0554	4.3622	-4.8464	0.1503	0.0177	0.0804	-3.4105	-4.8464	1.4359	0.1692
0.0058	-4.9174	-3.3951	1.5223	0.1794	0.0308	-4.1243	-3.3951	0.7292	0.0859	0.0558	5.0760	-3.3951	0.0154	0.0018	0.0808	-2.0848	-3.3951	1.3103	0.1544
0.0061	-4.2829	-1.7502	2.5327	0.2984	0.0311	-2.5380	-1.7502	0.7878	0.0928	0.0561	-7.6934	-1.7502	0.5118	0.0603	0.0811	-0.6345	-1.7502	1.1157	0.1315
0.0064	-2.5380	0.0000	2.5380	0.2991	0.0314	-1.6656	0	1.6656	0.1963	0.0564	-6.9795	0.0000	0.6345	0.0748	0.0814	0.3173	0.0000	0.3173	0.0374
0.0067	-0.7138	1.7502	2.4640	0.2903	0.0317	0.3966	1.7502	1.3537	0.1595	0.0567	-6.5037	1.7502	1.4330	0.1689	0.0817	2.5380	1.7502	0.7878	0.0928
0.0071	0.4759	3.3951	2.9192	0.3440	0.0321	2.5147	3.3951	0.8804	0.1037	0.0571	-5.9485	3.3951	1.0157	0.1197	0.0821	3.4898	3.3951	0.0947	0.0112
0.0074	2.3001	4.8464	2.5463	0.3000	0.0324	3.3311	4.8464	1.5152	0.1785	0.0574	-4.9967	4.8464	0.4842	0.0571	0.0824	5.4726	4.8464	0.6262	0.0738
0.0077	3.2518	6.0460	2.7942	0.3293	0.0327	4.6002	6.0460	1.4459	0.1704	0.0577	-3.4105	6.0460	0.9700	0.1143	0.0827	6.2657	6.0460	0.2197	0.0259
0.0080	4.8381	6.9720	2.1339	0.2514	0.0330	5.0760	6.9720	1.8959	0.2234	0.0580	6.3450	6.9720	0.6269	0.0739	0.0830	6.8209	6.9720	0.1510	0.0178
0.0083	6.0278	7.6359	1.6081	0.1895	0.0333	5.9485	7.6359	1.6874	0.1988	0.0583	6.9002	7.6359	0.7357	0.0867	0.0833	7.2968	7.6359	0.3391	0.0400
0.0087	6.6623	8.0743	1.4120	0.1664	0.0337	6.8209	8.0743	1.2533	0.1477	0.0587	7.6140	8.0743	0.4602	0.0542	0.0837	7.9313	8.0743	0.1430	0.0168
0.0090	7.5347	8.3349	0.8002	0.0943	0.0340	7.2175	8.3349	1.1174	0.1317	0.0590	8.0106	8.3349	0.3243	0.0382	0.0840	8.0899	8.3349	0.2450	0.0289
0.0093	8.0106	8.4625	0.4519	0.0533	0.0343	7.6934	8.4625	0.7692	0.0906	0.0593	8.1692	8.4625	0.2933	0.0346	0.0843	8.0899	8.4625	0.3726	0.0439
0.0096	8.3279	8.4865	0.1586	0.0187	0.0346	7.8520	8.4865	0.6345	0.0748	0.0596	8.1692	8.4865	0.3173	0.0374	0.0846	7.7727	8.4865	0.7138	0.0841
0.0099	8.3896	8.4130	0.0235	0.0028	0.0349	7.9313	8.4130	0.4817	0.0568	0.0599	7.8520	8.4130	0.5611	0.0661	0.0849	7.5347	8.4130	0.8783	0.1035
0.0103	8.0899	8.2238	0.1338	0.0158	0.0353	8.0106	8.2238	0.2132	0.0251	0.0603	7.3272	8.2238	0.8965	0.1056	0.0853	7.2968	8.2238	0.9270	0.1092
0.0106	7.8520	7.8804	0.0284	0.0033	0.0356	7.6934	7.8804	0.1870	0.0220	0.0606	6.9795	7.8804	0.9008	0.1061	0.0856	6.9002	7.8804	0.9801	0.1155
0.0109	7.2968	7.3348	0.0380	0.0045	0.0359	6.8209	7.3348	0.5139	0.0606	0.0609	6.6623	7.3348	0.6725	0.0792	0.0859	5.9485	7.3348	1.3864	0.1634
0.0112	6.5830	6.5432	0.0398	0.0047	0.0362	6.3904	6.5432	0.1528	0.0180	0.0612	5.5519	6.5432	0.9913	0.1168	0.0862	4.9967	6.5432	1.5465	0.1822
0.0115	5.5519	5.4799	0.0720	0.0085	0.0365	5.5519	5.4799	0.0720	0.0085	0.0615	4.9967	5.4799	0.4832	0.0569	0.0865	3.9656	5.4799	1.5142	0.1784
0.0119	4.0648	4.1494	0.0846	0.0100	0.0369	4.1243	4.1494	0.0251	0.0030	0.0619	3.0139	4.1494	1.1355	0.1338	0.0869	3.0139	4.1494	1.1355	0.1338
0.0122	3.2331	2.5919	0.6412	0.0756	0.0372	3.2518	2.5919	0.6599	0.0778	0.0622	1.5828	2.5919	1.0092	0.1189	0.0872	1.3483	2.5919	1.2436	0.1465
0.0125	2.4587	0.8819	1.5768	0.1858	0.0375	1.3483	0.8819	0.4664	0.0550	0.0625	0.7931	0.8819	0.0888	0.0105	0.0875	-0.5552	0.8819	1.4371	0.1693
0.0128	0.7931	-0.8819	1.6750	0.1974	0.0378	0.3173	-0.8819	1.1992	0.1413	0.0628	-0.7138	-0.8819	0.1681	0.0198	0.0878	-1.9035	-0.8819	1.0216	0.1204
0.0131	-0.9518	-2.5919	1.6402	0.1933	0.0381	-1.3483	-2.5919	1.2436	0.1465	0.0631	-2.0621	-2.5919	0.5298	0.0624	0.0881	-3.2360	-2.5919	0.6440	0.0759
0.0135	-1.9035	-4.1494	2.2459	0.2646	0.0385	-3.2518	-4.1494	0.8975	0.1058	0.0635	-3.7277	-4.1494	0.4217	0.0497	0.0885	-3.9114	-4.1494	0.2380	0.0280
0.0138	-3.4105	-5.4799	2.0694	0.2439	0.0388	-3.9656	-5.4799	1.5142	0.1784	0.0638	-5.1553	-5.4799	0.3246	0.0382	0.0888	-5.7898	-5.4799	0.3100	0.0365
0.0141	-3.9656	-6.5432	2.5775	0.3037	0.0391	-5.8692	-6.5432	0.6740	0.0794	0.0641	-5.6312	-6.5432	0.9120	0.1075	0.0891	-7.2175	-6.5432	0.6743	0.0795
0.0144	-5.5519	-7.3348	1.7829	0.2101	0.0394	-6.5830	-7.3348	0.7519	0.0886	0.0644	-6.5037	-7.3348	0.8312	0.0979	0.0894	-7.5347	-7.3348	0.1999	0.0236
0.0147	-6.7416	-7.8804	1.1388	0.1342	0.0397	-7.6934	-7.8804	0.1870	0.0220	0.0647	-6.9795	-7.8804	0.9008	0.1061	0.0897	-8.1692	-7.8804	0.2889	0.0340
0.0151	-6.9795	-8.2238	1.2442	0.1466	0.0401	-8.1692	-8.2238	0.0545	0.0064	0.0651	-7.6140	-8.2238	0.6097	0.0718	0.0901	-8.4072	-8.2238	0.1834	0.0216
0.0154	-7.4554	-8.4130	0.9576	0.1128	0.0404	-8.4072	-8.4130	0.0059	0.0007	0.0654	-7.6140	-8.4130	0.7990	0.0941	0.0904	-8.4865	-8.4130	0.0735	0.0087
0.0157	-7.5347	-8.4865	0.9518	0.1121	0.0407	-8.4865	-8.4865	0.0000	0.0000	0.0657	-7.6934	-8.4865	0.7931	0.0935	0.0907	-8.1692	-8.4865	0.3173	0.0374
0.0160	-8.1692	-8.4625	0.2933	0.0346	0.0410	-8.4072	-8.4625	0.0554	0.0065	0.0660	-7.4554	-8.4625	1.0071	0.1187	0.0910	-7.7727	-8.4625	0.6899	0.0813
0.0163	-8.4072	-8.3349	0.0723	0.0085	0.0413	-8.1692	-8.3349	0.1657	0.0195	0.0663	-7.3761	-8.3349	0.9588	0.1130	0.0913	-7.3761	-8.3349	0.9588	0.1130
0.0167	-8.0899	-8.0743	0.0157	0.0018	0.0417	-7.6140	-8.0743	0.4602	0.0542	0.0667	-7.1382	-8.0743	0.9361	0.1103	0.0917	-7.0589	-8.0743	1.0154	0.1197
0.0170	-7.4554	-7.6359	0.1805	0.0213	0.0420	-7.2175	-7.6359	0.4184	0.0493	0.0670	-6.2657	-7.6359	1.3702	0.1615	0.0920	-5.9485	-7.6359	1.6874	0.1988
0.0173	-7.2175	-6.9720	0.2455	0.0289	0.0423	-6.2657	-6.9720	0.7062	0.0832	0.0673	-5.7105	-6.9720	1.2614	0.1486	0.0923	-4.9174	-6.9720	2.0546	0.2421
0.0176	-6.5037	-6.0460	0.4576	0.0539	0.0426	-5.7105	-6.0460	0.3355	0.0395	0.0676	-4.9967	-6.0460	1.0493	0.1236	0.0926	-4.0450	-6.0460	2.0011	0.2358
0.0179	-5.3933	-4.8464	0.5469	0.0644	0.0429	-4.4415	-4.8464	0.4048	0.0477	0.0679	-4.3622	-4.8464	0.4842	0.0571	0.0929	-2.4587	-4.8464	2.3877	0.2813
0.0183	-4.7588	-3.3951	1.3637	0.1607	0.0433	-3.1725	-3.3951	0.2226	0.0262	0.0683	-2.0356	-3.3951	1.3594	0.1602	0.0933	-1.5863	-3.3951	1.8088	0.2131
0.0186	-2.3001	-1.7502	0.5498	0.0648	0.0436	-1.9828	-1.7502	0.2326	0.0274	0.0686	-0.8724	-1.7502	0.8778	0.1034	0.0936	0.4759	-1.7502	2.2261	0.2623
0.0189	-1.5069	-0.0000	1.5069	0.1776	0.0439	-0.6345	0.0000	0.6345	0.0748	0.0689	0	0.0000	0.0000	0.0000	0.0939	2.1414	0.0000	2.1414	0.2523
0.0192	0.0793	1.7502	1.6709	0.1969	0.0442	0.2379	1.7502	1.5123	0.1782	0.0692	1.9035	1.7502	0.1533	0.0181	0.0942	2.9346	1.7502	1.1843	0.1396
0.0196	1.7449	3.3951	1.6502	0.1945	0.0446	2.1414	3.3951	1.2536	0.1477	0.0696	2.8553	3.3951	0.5398	0.0636	0.0946	4.2829	3.3951	0.8878	0.1046
0.0199	2.4793	4.8464	2.3671	0.2789	0.0449	3.8070	4.8464	1.0394	0.1225	0.0699	4.4415	4.8464	0.4048	0.0477	0.0949	5.2347	4.8464	0.3883	0.0458
0.0202	4.0450	6.0460	2.0011	0.2358	0.0452	5.2347	6.0460	0.8114	0.0956	0.0702	6.0494	6.0460	0.0033	0.0004	0.0952	6.3450	6.0460	0.2990	0.0352
0.0205	4.8381	6.9720	2.1339	0.2514	0.0455	6.4243	6.9720	0.5476	0.0645	0.0705	6.5037	6.9720	0.4683	0.0552	0.0955	7.3761	6.9720	0.4041	0.0476
0.0208	6.4243	7.6359	1.2115	0.1428	0.0458	7.2175	7.6359	0.4184	0.0493	0.0708	7.0589	7.6359	0.5770	0.0680	0.0958	8.0899	7.6359	0.4540	0.0535
0.0212	7.1382	8.0743	0.9361	0.1103	0.0462	7.5347	8.0743	0.5395	0.0636	0.0712	7.3761	8.0743	0.6982	0.0823	0.0962	8.3279	8.0743	0.2536	0.0299
0.0215	7.4554	8.3349	0.8795	0.1036	0.0465	7.7727	8.3349	0.5622	0.0663	0.0715	8.0106	8.3349	0.3243	0.0382	0.0965	8.1692	8.3349	0.1657	0.0195
0.0218	7.9313	8.4625	0.5312	0.0626	0.0468	8.1692	8.4625	0.2933	0.0346	0.0718	8.0106	8.4625	0.4519	0.0533	0.0968	8.0106	8.4625	0.4519	0.0533
0.0221	7.9313	8.4865	0.5552	0.0654	0.0471	8.4865	8.4865	0.0000	0.0000	0.0721	8.1692	8.4865	0.3173	0.0374	0.0971	8.0899	8.4865	0.3966	0.0467
0.0224	7.9313	8.4130	0.4817	0.0568	0.0474	8.4865	8.4130	0.0735	0.0087	0.0724	7.3761	8.4130	1.0369	0.1222	0.0974	7.7727	8.4130	0.6404	0.0755
0.0228	7.5347	8.2238	0.6890	0.0812	0.0478	8.2485	8.2238	0.0248	0.0029	0.0728	7.2175	8.2238	1.0063	0.1186	0.0978	7.3761	8.2238	0.8477	0.0999
0.0231	7.1382	7.8804	0.7422	0.0875	0.0481	7.7727	7.8804	0.1077	0.0127	0.0731	6.7416	7.8804	1.1388	0.1342	0.0981	7.1382	7.8804	0.7422	0.0875
0.0234	6.5037	7.3348	0.8312	0.0979	0.0484	7.1382	7.3348	0.1967	0.0232	0.0734	5.9485	7.3348	1.3864	0.1634	0.0984	6.1864	7.3348	1.1484	0.1353
0.0237	6.2657	6.5432	0.2775	0.0327	0.0487	6.1071	6.5432	0.4361	0.0514	0.0737	5.0760	6.5432	1.4672	0.1729	0.0987	5.3140	6.5432	1.2292	0.1448
0.0240	5.2347	5.4799	0.2452	0.0289	0.0490	5.5519	5.4799	0.0720	0.0085	0.0740	3.8070	5.4799	1.6729	0.1971	0.0990	3.8070	5.4799	1.6729	0.1971
0.0244	4.5208	4.1494	0.3715	0.0438	0.0494	3.9656	4.1494	0.1837	0.0216	0.0744	2.7062	4.1494	1.4432	0.1701	0.0994	2.8553	4.1494	1.2941	0.1525
0.0247	3.2518	2.5919	0.6599	0.0778	0.0497	2.1671	2.5919	0.4248	0.0501	0.0747	1.4276	2.5919	1.1643	0.1372	0.0997	1.8401	2.5919	0.7519	0.0886
0.0250	1.6656	0.8819	0.7837	0.0923	0.0500	0.329	0.8819	0.5521	0.0651	0.0750	0.3966	0.8819	0.4853	0.0572	0.1000	1.4947	0.8819	0.6128	0.0722

References

[1] Kara, S., (Ed.). (2011). *Electromotive Force and Measurement in Several Systems*. IntechOpen. https://doi.org/10.5772/2109

[2] Yucai W., & Yonggang, L. (2016). Diagnosis of short circuit faults within turbogenerator excitation winding based on the expected electromotive force method. *IEEE Transactions on Energy Conversion*, *31*(2), 706 – 713. https://doi.org/10.1109/tec.2016.2521422

[3] Hao, L., Lin, M., Zhao, X., & Luo, H. (2011, August). Analysis and optimization of EMF waveform of a novel axial field flux-switching permanent magnet machine. In *2011 International Conference on Electrical Machines and Systems* (pp. 1-6). IEEE. https://doi.org/10.1109/icems.2011.6073668

[4] Wu, J., Deng, Z., Wang, C., & Sun, X. (2016, November). A new sensorless control method for PM machine with 180 degree commutation. In *2016 19th International Conference on Electrical Machines and Systems (ICEMS)* (pp. 1-5). IEEE.

[5] Hongsheng, H., & Weiguo, L. (2015, October). Research of Speed-torque characteristics of brushless DC motor based on back electromotive force. In *2015 18th International Conference on Electrical Machines and Systems (ICEMS)* (pp. 1301-1306). IEEE. https://doi.org/10.1109/icems.2015.7385240

[6] Dughiero, F., Forzan, M., Lupi, S., & Zerbetto, M. (2018, June). Induction Heating with Rotating Permanent Magnets: Experimental Results on an Industrial Installation. In *2018 19th International Conference of Young Specialists on Micro/Nanotechnologies and Electron Devices (EDM)* (pp. 1-7). IEEE. https://doi.org/10.1109/edm.2018.8435004

[7] Aliferov, A., Promzelev, V., Vlasov, D., Morev, A. & Bikeev, R. (2017). Induction heating based on permanent magnets with magnetic field concentrators. *Advances in Engineering Research*, *133*, 495-499. https://doi.org/10.2991/aime-17.2017.80

[8] Bojarevics, A. & Beinerts, T. (2010). Experiments on liquid metal flow induced by a rotating magnetic dipole. *Magnetohydrodynamics*, *46*(4), 333-338. https://doi.org/10.22364/mhd.46.4.2

[9] Zerbetto, M., Forzan, M., & Dughiero, F. (2015). Permanent magnet heater for a precise control of temperature in aluminum billets before extrusion. *Materials Today: Proceedings*, *2*(10), 4812-4819. https://doi.org/10.1016/j.matpr.2015.10.019

[10] Lee, S. J., Kenkel, J. M., Pecharsky, V. K., & Jiles, D. C. (2002). Permanent magnet array for the magnetic refrigerator. *Journal of Applied Physics*, *91*(10), 8894-8896. https://doi.org/10.1063/1.1451906

[11] Bjørk, R., Nielsen, K. K., Bahl, C. R., Smith, A., & Wulff, A. C. (2016). Comparing superconducting and permanent magnets for magnetic refrigeration. *AIP Advances*, *6*(5), 056205. https://doi.org/10.1063/1.4943305

[12] Bouchekara, H. R. E. H., Simsim, M. T., Boucherma, M., & Allag, H. (2012). Multiphysics modeling of a magnetic refrigeration system based on superconductors. *Progress In Electromagnetics Research M*, *23*, 229-247. https://doi.org/10.2528/PIERM11111608

[13] Dughiero, F., Forzan, M., Lupi, S., Nicoletti, F. & Zerbetto, M. (2011). A new high efficiency technology for the induction heating of nonmagnetic billets. *The International Journal of Computation and Mathematics in Electrical and Electronic Engineering*, *30*(5), 1528-1538. https://doi.org/10.1108/03321641111152685

[14] Karban, P., Mach, F., & Dolezel, I. (2012). Hard-coupled nonlinear model of induction heating of nonmagnetic cylindrical billets in rotation. *COMPEL - The International Journal of Computation and Mathematics in Electrical and Electronic Engineering*, *31*(3), 1368-1378. https://doi.org/10.1108/03321641211247841

[15] Ivo, D., Pavel, K., & Frantisek, M. (2014). Induction heating of rotating nonmagnetic billet in magnetic field produced by high-parameter permanent magnets. *Electrical Engineering and Electromechanics*, *2*, 32-36. https://doi.org/10.20998/2074-272x.2014.2.07

[16] Mach, F., Karban, P., & Doležel, I. (2012). Induction heating of cylindrical nonmagnetic ingots by rotation in static magnetic field generated by permanent magnets. *Journal of Computational and Applied Mathematics*, *236*(18), 4732-4744. https://doi.org/10.1016/j.cam.2012.02.035

[17] Allag, H., Yonnet, J. P., & Latreche, M. E. (2009, July). 3D analytical calculation of forces between linear Halbach-type permanent-magnet arrays. In *2009 8th International Symposium on*

Advanced Electromechanical Motion Systems & Electric Drives Joint Symposium (pp. 1-6). IEEE. https://doi.org/10.1109/ELECTROMOTION.2009.5259084

[18] Allag, H. (2010). *Modeles et Calcul des Systemes de Suspension Magnetique Passive-Developpements et Calculs Analytiques en 2D et 3D des Interactions entre Aimants Permanents*. [Doctoral dissertation, Université de Grenoble]. https://tel.archives-ouvertes.fr/tel-00569274

[19] Zhao, L. Z., Peng, Y., Sha, C. W., Li, R., & Xu, Y. Y. (2010). Permanent Magnet Type Eddy Current Heater Based on Cylindrical Halbach Array for Reducing Oil's Viscosity. *IEEE Transactions on Applied Superconductivity*, *20*(3), 865-869. https://doi.org/10.1109/tasc.2009.2038932

[20] Mach, F., Štarman, V., Karban, P., Doležel, I., & Kůs, P. (2013). Finite-element 2-D model of induction heating of rotating billets in system of permanent magnets and its experimental verification. *IEEE Transactions on Industrial Electronics*, *61*(5), 2584-2591. https://doi.org/10.1109/TIE.2013.2276025

[21] Karban, P., Doležel, I., Mach, F., & Ulrych, B. (2013). Advanced adaptive algorithms in 2D finite element method of higher order of accuracy. *COMPEL-The international journal for computation and mathematics in electrical and electronic engineering*, *32*(3), 834-849. https://doi.org/10.1108/03321641311305782

[22] Allag, H., Yonnet, J. P., Bouchekara, H. R., Latreche, M. E., & Rubeck, C. (2015). Coulombian model for 3D analytical calculation of the torque exerted on cuboidal permanent magnets with arbitrary oriented polarizations. *The Applied Computational Electromagnetics Society Journal (ACES)*, *30*(4). 351-356. https://journals.riverpublishers.com/index.php/ACES/article/view/10551

[23] Yonnet, J. P. & Allag, H. (2011). Three-Dimensional Analytical Calculation of Permanent Magnet Interactions by "Magnetic Node" Representation. *IEEE Transactions on Magnetics*, *47*(8). 2050-2055. https://doi.org/10.1109/TMAG.2011.2122339

[24] Allag, H., Yonnet, J. P., Fassenet, M., & Latreche, M. E. (2009). 3D analytical calculation of interactions between perpendicularly magnetized magnets—Application to any magnetization direction. *Sensor Letters*, *7*(3), 486-491. https://doi.org/10.1166/sl.2009.1094

[25] Allag, H., & Yonnet, J. P. (2009). 3-D analytical calculation of the torque and force exerted between two cuboidal magnets. *IEEE Transactions on Magnetics*, *45*(10), 3969-3972. https://doi.org/10.1109/TMAG.2009.2025047

[26] Allag, H., & Yonnet, J. P. (2013). Analytical Calculation of the Torque Exerted Between Two Permanent Magnets, *Sensor Letters*, *10*(1), 141-144. https://doi.org/10.1166/sl.2013.2775

[27] Allag, H., Yonnet, J. P., & Latreche, M. E. (2011). Analytical calculation of the torque exerted between two perpendicularly magnetized magnets. *Journal of Applied Physics*, *109*(7), 07E701. https://doi.org/10.1063/1.3535148

[28] Post, R. F., & Ryutov, D. D. (2000). The Inductrack: a simpler approach to magnetic levitation, *IEEE Transactions on Applied Superconductivity*, *10*(1), 901-904. https://doi.org/10.1109/77.828377

[29] Ravaud, R., & Lemarquand, G. (2009). Magnetic couplings with cylindrical and plane air gaps: Influence of the magnet polarization direction. *Progress In Electromagnetics Research B*, *16*, 333-349. https://doi.org/10.2528/PIERB09051903

[30] Yonnet, J. P. (1978). Passive magnetic bearings with permanent magnets. *IEEE Transactions on Magnetics*, *14*(5), 803 – 805. https://doi.org/10.1109/TMAG.1978.1060019

[31] Takabayashi, H., & Okada, S. (1989). Development of a permanent magnet for a high performance undulator. *Review of Scientific Instruments*, *60*(7), 1842-1844. https://doi.org/10.1063/1.1140918

[32] French, C., & Acarnley, P. (1996). Control of permanent magnet motor drives using a new position estimation technique. *IEEE Transactions on Industry Applications*, *32*(5), 1089-1097.. https://doi.org/10.1109/28.536870

[33] Reigosa, D. D., Fernandez, D., Tanimoto, T., Kato, T., & Briz, F. (2016). Permanent-magnet temperature distribution estimation in permanent-magnet synchronous machines using back electromotive force harmonics. *IEEE Transactions on Industry Applications*, *52*(4), 3093-3103. https://doi.org/10.1109/TIA.2016.2536579

[34] De Bisschop, J., Vansompel, H., Sergeant, P., & Dupre, L. (2017). Demagnetization fault detection in axial flux PM machines by using sensing coils and an analytical model. *IEEE Transactions on Magnetics*, *53*(6), 1-4. https://doi.org/10.1109/TMAG.2017.2669480

[35] Djemoui, S., Allag, H., Chebout, M. & Bouchekara, H. (2021). Partial Electrical Equivalent Circuits and Finite Difference Methods Coupling; Application to Eddy Currents Calculation for Conductive and Magnetic Thin Plates. *Progress in Electromagnetics Research C*, *114*, 83-96. https://doi.org/10.2528/PIERC21051602

Riad Bouakacha received his engineering degree in electrical engineering with a major in electrical networks from the University of Jijel and his degree of magister in modeling and simulation of industrial electrical installations at the University of Skikda in 2009. Currently, he is working on heating systems with magnetic induction based on permanent magnets

Mehdi Ouili received the B.S. and M.S. degrees in Electrical Engineering from the University of Constantine, Algeria in 2010 and 2013 respectively. He is currently working toward a Ph.D. degree at the Department of Electrical Engineering of the same university. He is also a member of the LEC laboratory staff. His current research interests include magnetic separation process.

Hicham Allag received a diploma in Electrical Engineering from the University of Jijel (Algeria) and the magister from the University of Constantine respectively in 2000 and 2002. He was qualified as Assistant Professor at Jijel University in 2003. In 2010, he received the PhD from the University of Joseph Fourier in France. He is currently a Professor at the University of Jijel, Director of the Electrotechnical and Industrial Electronic Laboratory, Head of Department of Fundamental Sciences and Technology. His scientific researches include computational electromagnetic and control applications.

Rabia Mehasni received his Ph.D. in Electrical Engineering from the University of Constantine 1, Algeria, in 2007. He has been with the Department of Electrical Engineering, the University of Constantine 1 since 2000. He is currently the Research Director at the LEC Laboratory. He has published in the field of magnetic separation. His research interests are numerical methods and modeling techniques in multidisciplinary problems.

Mohammed Chebout received the engineer degree in Electrical Engineering from the Institute of Science and Technology of the University of Jijel, Algeria in 2003. In 2019, He received his Ph.D. in Electrical Engineering from the same university and joined the research team of the Applied Automation and Industrial Diagnostics Laboratory. His research interest focus on finding new algorithms and optimization methods for the diagnosis and identification of crack forms based on different NDT techniques.

Houssem R. E. H. Bouchekara is an Associate Professor at the Electrical Engineering Department of the University of Hafr Al Batin. He received his B.S. in Electrical Engineering from the University of Constantine 1, Algeria, in 2004. He received his Master in Electronic Systems and Electrical Engineering from the Polytechnic School of the University of Nantes, France, 2005. He received his Ph.D. in Electrical Engineering from the Grenoble Institute of Technology, France, in 2008. His research interests include optimization techniques, magnetic refrigeration, electromagnetics, electric machines and power systems.